JOURNAL OF THE KOREAN ASTRONOMICAL SOCIETY
32: 1 ∼ , 1999

NUMERICAL SIMULATIONS OF INCOMPRESSIBLE MHD TURBULENCE

JUNGYEON CHO
475 N. Charter St., Department of Astronomy, Univ. of Wisconsin, Madison, WI53706, USA; cho@astro.wisc.edu
(Received ???. ??, 2001; Accepted ???. ??,2001)

ABSTRACT

The study of incompressible magnetohydrodynamic (MHD) turbulence gives useful insights on many astrophysical problems. We describe a pseudo-spectral MHD code suitable for the study of incompressible turbulence. We review our recent works on direct three-dimensional numerical simulations for MHD turbulence in a periodic box. In those works, we use a pseudo-spectral code to solve the incompressible MHD equations. We first discuss the structure and properties of turbulence as functions of scale. The results are consistent with the scaling law recently proposed by Goldreich & Sridhar. The scaling law is based on the concept of scale-dependent isotropy: smaller eddies are more elongated than larger ones along magnetic field lines. This scaling law substantially changes our views on MHD turbulence. For example, as noted by Lazarian & Vishniac, the scaling law can provide a fast reconnection rate. We further discuss how the study of incompressible MHD turbulence can help us to understand physical processes in interstellar medium (ISM) by considering imbalanced cascade and viscous damped turbulence.

Key Words : ISM:general-MHD-turbulence

I. INTRODUCTION

Astrophysical flows are complicated and dynamic. For example, molecular clouds are clumpy over a vast range of scales and observations of velocity spectral line broadening indicate that dynamic pressure ($\rho\,\mathbf{v}^2/2$) usually dominates the thermal pressure (nkT). Furthermore, velocity spectral lines show multiple components. These facts suggest that cloud internal velocity possesses disordered components. In molecular clouds, the characteristic Reynolds number is estimated to be larger than $\sim 10^{10}$, which is consistent with the turbulent state in the clouds. In general, when the Reynolds number ($\equiv LV/\nu$; L=characteristic size of the system, V=velocity dispersion, and ν=viscosity) is larger than an order of 10 - 100, the system becomes unstable and turbulent.

In laboratory systems, fluids are usually incompressible and unmagnetized. Kolmogorov phenomenology provides an excellent insight for such systems. Suppose that we 'disturb' the fluid at a scale L. We call this scale as *energy injection scale* or *largest energy containing eddy scale*. Then the energy injected to the scale L cascades to progressively smaller and smaller scales. Ultimately, the energy will reach the molecular dissipation scale l_d and it will be lost there. The scales between L and l_d is called the *inertial range*. Suppose a scale l lies in the inertial range. Let the characteristic velocity associated with the scale be v_l. Kolmogorov theory states that the kinetic energy (v_l^2) is transferred to one-level smaller scale within one eddy turnover time (l/v_l). It is natural that the cascade rate ($v_l^2/(l/v_l)$) be scale-independent. Therefore, we have

$$v_l \propto l^{1/3}. \tag{1}$$

(One-dimensional) Energy spectrum $E(k)$ is one of the most important quantities in turbulence theories. Note that $E(k)dk$ is the amount of energy between the wavenumber k and $k+dk$. When $E(k)$ follows a power law, $kE(k)$ is the energy *near* the wavenumber $k \sim 1/l$. Since v_l^2 represents a similar energy, we have $v_l^2 \approx kE(k)$. Therefore, equation (1) becomes

$$E(k) \propto k^{-5/3}. \tag{2}$$

This is the well-known Kolmogorov spectrum. Astrophysical fluids are compressible and magnetized. Nevertheless, many astrophysical quantities follow this Kolmogorov spectrum. It is important to note that Kolmogorov theory predicts: 1. the velocity dispersion ($\sim v_l$) decreases with scales as $v_l \propto l^{1/3}$; 2. the slope of the energy spectrum is $-5/3$.

Earlier works on ISM focused on the velocity dispersions and derived a qualitative agreement with the Kolmogorov theory. Larson (1981) and Myers (1983) found that velocity dispersion decreases as the size of the clumps decreases, which may support turbulent model of ISM. Scalo (1984) showed that two-point velocity correlation increases as the separation decreases, which is also qualitatively consistent with turbulent model. All the above mentioned studies are for scales larger than or similar to ~ 1 pc.

On the other hand, other studies address the issue of power spectra. Interstellar scintillation observations indicate electron density spectrum follows a power law over 7 decades of length scales (see Armstrong et al. 1995). The slope of the spectrum is very close to $-5/3$ for $10^6 m$ - $10^{14} m$. The spectrum is somewhat uncertain for scales larger than $10^{14} m$ ($\sim 0.01 pc$). However, recently, Lazarian & Pogosyan (2000) and Starnimirovic & Lazarian (2001) showed the existence of the $-5/3$ velocity power spectrum over pc-scales in HI. Solar-wind observations provide *in-situ* measurements of the power spectrum of magnetic fluctuations. Leamon et

al. (1998) obtained a slope of -1.7.

Therefore it is evident that turbulence is prevalent in astrophysical fluids. Understanding the nature of such turbulence is important because it affects many astrophysical processes. For example, star formation rate depends on the turbulence decay time-scale. Heat and cosmic ray transport also depend on the statistics of turbulence. Recently anisotropic MHD Turbulence has also been evoked to provide fast magnetic reconnection rate (Lazarian & Vishniac 1999).

One approach to studying the ISM is to perform time-dependent numerical simulations to model the ISM, including as many of the interacting phenomena as practical. Of course, the physics included in such models must necessarily be highly simplified, and it is difficult to determine which features of the final model result from which physical assumptions (or initial conditions). Our approach is to use simplified numerical simulations to study the influences of various physical phenomena in isolation. We want to obtain a physical feeling for the general effects that each phenomenon has on the nature of the ISM. Here we review our previous works on incompressible MHD turbulence. It is obvious that the real ISM is compressible, but we want to separate the effects of magnetic turbulence from those involving compression. In later works we will include compression for comparison with the present models, thereby isolating its importance directly.

As we said earlier, we will numerically study incompressible MHD turbulence. We believe Fourier spectral method is one of the best numerical methods for such calculations. In II, we show how the spectral method works. In III, we introduce our recent works done with the spectral code: anisotropy, decay speed of MHD turbulence, and magnetic structures below the viscous cutoff. In IV, we give conclusion.

II. NUMERICAL METHOD

(a) PSEUDO-SPECTRAL METHOD

For simplicity, let us first consider incompressible *unmagnetized* fluid. Then, the governing equation is the Navier-Stocks equation:

$$\frac{\partial \mathbf{v}}{\partial t} = -\nabla \cdot (\mathbf{vv}) + \nu \nabla^2 \mathbf{v} + \nabla P, \tag{3}$$

where $\mathbf{v}$ is velocity, ν is viscosity, and P is gas pressure. Since we are considering an incompressible fluid, we can assume that $\rho = 1$.

The Fourier spectral method is highly suitable for incompressible flows. Simply put, the idea of the method is simple: we transform all physical space variables into Fourier (or wave-vector) space and solve the differential equation there. Hereafter, we assume that we are solving the equation on a uniform rectangular grid. Some advantage of the method is:

1. It shows fast convergence for smooth functions.
2. It is easy to implement divergence-free conditions.
3. It is easy to implement periodic boundary condition.
4. Fourier space analyses (e.g. calculation of energy spectrum) are natural consequences.

We note that the gradient operator becomes $i\mathbf{k}$ and that multiplication becomes convolution sum in Fourier space. Here $i = \sqrt{-1}$. Using these facts, we obtain the Navier-Stocks equation in Fourier space:

$$\frac{\partial \hat{\mathbf{v}}(\mathbf{k})}{\partial t} = -i\mathbf{k} \cdot (\widehat{\mathbf{vv}})(\mathbf{k}) - i\nu k^2 \hat{\mathbf{v}}(\mathbf{k}) + i\mathbf{k}\hat{P}(\mathbf{k}), \tag{4}$$

where

$$(\widehat{\mathbf{vv}})(\mathbf{k}) \equiv \int_{\mathbf{p}+\mathbf{q}=\mathbf{k}} d\mathbf{k}\ \hat{\mathbf{v}}(\mathbf{p})\hat{\mathbf{v}}(\mathbf{q}). \tag{5}$$

The incompressibility condition becomes

$$i\mathbf{k} \cdot \hat{\mathbf{v}}(\mathbf{k}) = 0, \tag{6}$$

which means that the velocity vector stays perpendicular to the wave vector $\mathbf{k}$. Since the pressure term in equation (4) is parallel to $\mathbf{k}$, we can drop the term. On the other hand, the nonlinear term (i.e the term containing $\widehat{\mathbf{vv}}$) may have both parallel and perpendicular components. Therefore, we need to remove the component parallel to $\mathbf{k}$ by applying an appropriate projection operator.

The calculation of the nonlinear term is the most time consuming part of the Fourier spectral methods. For simplicity, let us consider the following one dimensional convolution sum:

$$\int_{p+q=k} dk\ \hat{f}(p)\hat{g}(q). \tag{7}$$

Then the discrete representation of the convolution sum is

$$\sum_{p+q=k} \hat{f}_p \hat{g}_q. \tag{8}$$

The pseudo-spectral method approximates the convolution sum as

$$\sum_{p+q=k} \hat{f}_p \hat{g}_q \approx \left[F^{-1} \left[F(\hat{f}) F(\hat{g}) \right] \right]_k, \tag{9}$$

where F and F^{-1} denote forward/inverse Fourier transform. The cost of such calculation is $O(N \log N)$, where N is the number of grid points.

Once we obtain the convolution sum, we can use any techniques for *ordinary* differential equations to solve the time evolution of the Navier-Stocks equation.

(b) ACTUAL SETUP

In actual calculations, we have adopted a pseudospectral code and calculated the time evolution of incompressible magnetic turbulence subject to a random driving force per unit mass:

$$\frac{\partial \mathbf{v}}{\partial t} = (\nabla \times \mathbf{v}) \times \mathbf{v} - (\nabla \times \mathbf{B}) \times \mathbf{B} + \nu \nabla^2 \mathbf{v} + \mathbf{f} + \nabla P', \tag{10}$$

$$\frac{\partial \mathbf{B}}{\partial t} = \nabla \times (\mathbf{v} \times \mathbf{B}) + \eta \nabla^2 \mathbf{B}, \tag{11}$$

$$\nabla \cdot \mathbf{v} = \nabla \cdot \mathbf{B} = 0, \tag{12}$$

where $\mathbf{f}$ is a random driving force, $P' \equiv P/\rho + \mathbf{v} \cdot \mathbf{v}/2$, $\mathbf{v}$ is the velocity, and $\mathbf{B}$ is magnetic field divided by $(4\pi\rho)^{1/2}$. In this representation, $\mathbf{v}$ can be viewed as the velocity measured in units of the r.m.s. velocity, v, of the system and $\mathbf{B}$ as the Alfven speed in the same units. The time t is in units of the large eddy turnover time ($\sim L/v$) and the length in units of L, the inverse wavenumber of the fundamental box mode. In this system of units, the viscosity ν and magnetic diffusivity η are the inverse of the kinetic and magnetic Reynolds numbers respectively. The turbulence is driven by 21 random forcing components in Fourier space. The peak of energy injection occurs at $k \approx 2.5$. The amplitudes of the forcing components are tuned to ensure $v \approx 1$ We use exactly the same forcing terms for all simulations. We use up to 256^3 collocation points. We use an integration factor technique for kinetic and magnetic dissipation terms and a leap-frog method for nonlinear terms. At $t = 0$, the magnetic field has only its uniform component and the velocity field is restricted to the range $2 \leq k \leq 4$ in wavevector space.

For some runs, we use hyperviscosity and hyperdiffusivity for the dissipation terms. The power of hyperviscosity is set to either 2 or 8, so that the dissipation term in the above equation is replaced with

$$-\nu_h (\nabla^2)^h \mathbf{v}, \tag{13}$$

where $h = 2$ or 8. A similar expression is used for the magnetic dissipation term. In subsections III(a) and III(b), we use unit magnetic Prandtl number ($\nu = \eta$) and the notation NY-B_0Z. In subsection III(c), we use physical viscosity and physical- or hyper-diffusion and the notation NXY-B_0Z. Here N = 256, 144 refers to the number of grid points in each spatial direction; X = P refers to physical viscosity; Y = P, H2, H8 refers to the form of diffusion (physical-, the 2nd power hyper-, or the 8th power hyper-diffusion, respectively); Z=0.5 or 1 refers to the strength of the external magnetic field in Alfven velocity unit.

Diagnostics for our code can be found in Cho and Vishniac (2000b).

III. PROPERTIES OF MHD TURBULENCE

In this section, we discuss the properties of MHD turbulence in the presence of a strong uniform background field.

(a) ANISOTROPY

Historically hydrodynamic turbulence in an incompressible fluid was successfully described by the eddy cascade (Kolmogorov 1941), but MHD turbulence was first modeled by wave turbulence (Iroshnikov 1963, Kraichnan 1965). This theory assumes isotropy of the energy cascade in Fourier space. However, the magnetic field defines a local symmetry axis since it is easy to mix field lines in directions perpendicular to the local $\mathbf{B}$ and much more difficult to bend them. In a turbulent medium, the kinetic energy associated with large scale motions is greater than that of small scales. However, the strength of the local mean magnetic field is almost the same on all scales. Therefore, it becomes relatively difficult to bend magnetic field lines as we consider smaller scales, leading to more pronounced anisotropy. A self-consistent model of MHD turbulence which incorporates this concept of scale dependent anisotropy was introduced by Goldreich & Sridhar (1995; hereinafter GS95).

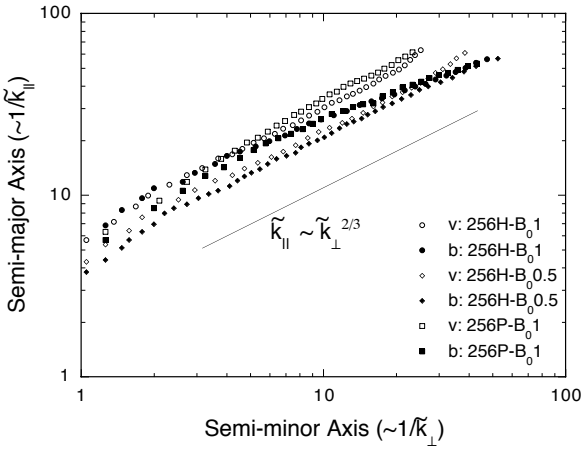

Fig. 1.— The relation between $k_\parallel$ and $k_\perp$. (Cho & Vishniac 2000a).

The major predictions of the GS95 model are as follows. First, anisotropy is scale dependent. Roughly speaking, the semi-major axis ($1/k_\parallel$) and the semi-minor axis ($1/k_\perp$) of an eddy satisfy the relation $k_\parallel \propto k_\perp^{2/3}$, which means smaller eddies are relatively more elongated than larger ones. Here $k_\perp$ and $k_\parallel$ are wave numbers perpendicular and parallel to the background field. Second, the model predicts that the one-dimensional energy spectrum is Kolmogorov-type if expressed in terms of perpendicular wavenumbers, i.e. $E(k_\perp) \propto k_\perp^{-5/3}$.

Numerical simulations by Cho & Vishniac (2000a) and Maron & Goldreich (2001) have mostly supported the GS95 model and helped to extend it. Both analyses stressed the point that scale dependent anisotropy can be measured only in local coordinate frames which are aligned with the locally averaged magnetic field direction. Cho & Vishniac (2000a) calculated the structure functions of velocity and magnetic field in the local frames, and found that the contours of the structure functions do show scale dependent anisotropy, consistent with the predictions of the GS95 model. Fig 1. shows that the semi-major axis ($1/k_\parallel$) is proportional to the 2/3 power of the semi-minor axis ($1/k_\perp$), imply-

ing that $k_\parallel \propto k_\perp^{2/3}$. One dimensional energy spectrum follows Kolmogorov spectrum: $E(k) \propto k^{-5/3}$ (see Cho & Vishniac 2000a).

(b) DECAY OF MHD TURBULENCE

Turbulence plays a critical role in molecular cloud support and star formation and the issue of the time scale of turbulent decay is vital for understanding these processes.

If MHD turbulence decays quickly then serious problems face researchers attempting to explain important observational facts, i.e. turbulent motions seen within molecular clouds without star formation (see Myers 1999) and rates of star formation (Mckee 2000). Earlier studies attributed the rapid decay of turbulence to compressibility effects (Mac Low 1999). Cho et al. (2001), as well as earlier ones (Cho & Vishniac 2000a, Maron & Goldreich 2001), shows that turbulence decays rapidly even in the incompressible limit. This can be understood in the framework of GS95 model where mixing motions perpendicular to magnetic field lines form hydrodynamic-type eddies. Such eddies, as in hydrodynamic turbulence, decay in one eddy turnover time.

Below we consider the effect of imbalance on the turbulence decay time scale. MHD turbulence can be described by opposite-traveling wave packets. 'Imbalance' means that wave packets traveling in one direction have significantly larger amplitudes than the other. In astronomy, many energy sources are localized. For example, SN explosions and OB winds are typical point energy sources. Furthermore, astrophysical jets from YSOs are believed to be highly collimated. With these localized energy sources, it is natural to think that interstellar turbulence is typically imbalanced.

In this subsection, we explicitly relate the degree of imbalance and the decay time scale of turbulence in the presence of a strong uniform background field.

In Figure 2 we demonstrate that an imbalanced cascade does extend the lifetime of MHD turbulence. We use the run 144H-$B_0$1 to investigate the decay time scale. We ran the simulation up to t=75 with non-zero driving forces. Then at t=75, we turned off the driving forces and let the turbulence decay. At t=75, there is a slight imbalance between upward and downward moving components ($E_+ = 0.499$ and $E_- = 0.40$). This results from a natural fluctuation in the simulation. The case of $(E_+)_{t_0} = 80\%(E_-)_{t_0}$ corresponds to the simulation that starts off from this initial imbalance. In other cases, we either increase or decrease the energy of $\mathbf{z}^-$ components and, by turning off the forcing terms, let the turbulence decay. We can clearly observe that imbalanced turbulence extends the decay time scale substantially. Note that we normalized the initial energy to 1. The y-axis is the total (=up + down) energy.

In this section, we found that turbulence decay time can be slow. If we consider the interstellar medium at

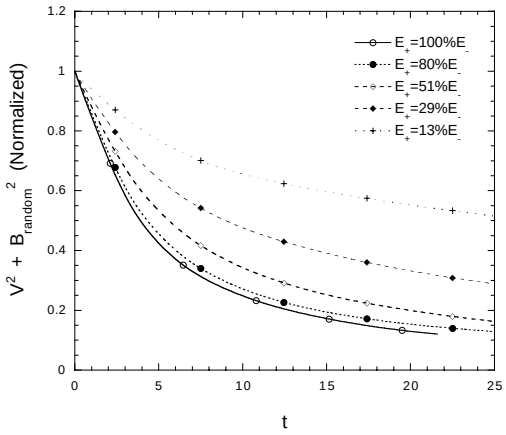

Fig. 2.— Decay of imbalanced turbulence. Imbalanced cascade can extend decay time. Run 144H-$B_0$1. (Cho et al. 2001)

larger scales, it is definitely compressible, has a whole range of energy injection/dissipation scales (see Scalo 1987), and the relative role of vortical versus compressible motions being unclear. Nevertheless, we believe that our simplified treatment may still elucidate some of the basic processes. To what extend this claim can be justified will be clear when we compare compressible and incompressible results. However, if we accept that fast and slow MHD modes are subjected to fast collisionless damping (see Minter & Spangler 1997) the remaining modes are incompressible Alfven modes. Those should be well described by our model when turbulence is supersonic but sub-Alfvenic. Our preliminary results (Cho & Lazarian 2002) show that the coupling of the modes is marginal even in compressible regime.

(c) STRUCTURES BELOW VISCOUS CUTOFF

In hydrodynamic turbulence viscosity sets a minimal scale for motion, with an exponential suppression of motion on smaller scales. Below the viscous cutoff the kinetic energy contained in a wavenumber band is dissipated at that scale, instead of being transferred to smaller scales. This means the end of the hydrodynamic cascade, but in MHD turbulence this is not the end of magnetic structure evolution. For viscosity much larger than resistivity, $\nu \gg \eta$, there will be a broad range of scales where viscosity is important but resistivity is not. On these scales magnetic field structures will be created through a combination of large scale shear and the small scale motions generated by magnetic tension. As a result, we expect a power-law tail in the energy distribution, rather than an exponential cutoff. To our best knowledge, this is a completely new regime of MHD turbulence. Ambipolar diffusion damps turbulent motions in ISM. Therefore, the study of such a viscous damped MHD turbulence is particu-

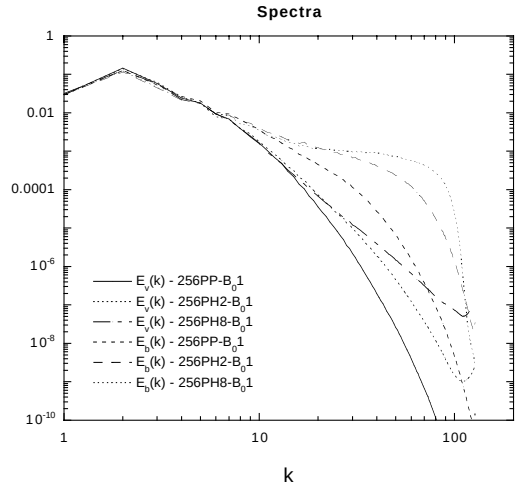

Fig. 3.— Energy spectra at t=15. From Cho et al. 2002.

larly important for many astrophysical processes below the ambipolar diffusion scale in ISM.

In Cho, Lazarian, & Vishniac (2002), we numerically demonstrate the existence of the power-law magnetic energy spectrum below the viscous damping scale. We use the same pseudo-spectral incompressible MHD code. We use physical viscosity for velocity. The kinetic Reynolds number is around 100. We use three different values of magnetic diffusion: physical diffusion, hyper-diffusion with order 2, and hyper-diffusion with order 8. We will present a theoretical model for this regime in an upcoming paper (Lazarian, Vishniac, & Cho 2002).

In Figure 3, we plot energy spectra. The spectra consist of several parts. First, the peak of the spectra corresponds to the energy injection scale. Second, for $2 < k < 6$, kinetic and magnetic spectra follow a similar slope. This part may be the short inertial range in general sense. Third, magnetic and kinetic spectra decouple at $k \sim 6$. Forth, for $20 < k$, it appears that a new damped-scale inertial range emerges. The emergence of the new inertial range is conspicuous in the order 8 hyperdiffusion simulation.

IV. SUMMARY

We described a pseudo-spectral MHD code and demonstrated its usefulness in astrophysics through our recent works. We showed that the rate at which MHD turbulence decays depends on the degree of energy imbalance between wave packets traveling in opposite directions. A substantial degree of imbalance can substantially extend the decay time scale of the MHD turbulence, which might be useful for the study of star formation. We also showed that magnetic fields can have rich structures below the viscous cut-off scale, which implies that magnetic fields have stochastic structures below the ambipolar diffusion scale in ISM and, therefore, affect many astrophysical processes, such as cosmic ray transports, magnetic reconnection, and thermal diffusion.

ACKNOWLEDGEMENTS

I thank Alex Lazarian, Ethan T. Vishniac, and Peter Goldreich for valuable discussions. The introduction of this proceeding is partly based on email communication with John Scalo. This work was partially supported by National Computational Science Alliance under CTS980010N and AST000010N and utilized the NCSA SGI/CRAY Origin2000.

REFERENCES

Armstrong, J. W., Rickett, B. J., & Spangler, S. R. 1995, ApJ, 443, 209

Cho, J. & Vishniac, E. T. 2000a, ApJ, 539, 273

Cho, J. & Vishniac, E. T. 2000b, ApJ, 538, 217

Cho, J., Lazarian, A., & Vishniac, E. T. 2001, ApJ, in press

Cho, J. & Lazarian, A. 2002, in preparation

Cho, J., Lazarian, A., & Vishniac, E. T. 2002, in preparation

Goldreich, P. & Sridhar, H. 1995, ApJ, 438, 763 (GS95)

Iroshnikov, P. 1963, Astron. Zh., 40, 742 (English version: 1964, Sov. Astron., 7, 566)

Kolmogorov, A. 1941, Dokl. Akad. Nauk SSSR, 31, 538

Kraichnan, R. 1965, Phys. Fluids, 8, 1385

Larson, R. B. 1981, MNRAS, 194, 809

Lazarian, A. & Pogosyan, D. 2000, ApJ, 537, 720L

Lazarian, A.& Vishniac, E. T. 1999, ApJ, 517, 700

Lazarian, A.& Vishniac, E. T., & Cho, J. 2002, in preparation

Leamon, R. J., Smith, C. W., Ness, N. F., & Matthaeus, W. H. 1998, J. Geophys. Res., 103, 4775

Mac Low, M. 1999, ApJ, 524, 169

Maron, J. & Goldreich, P. 2001, ApJ, 554, 1175

McKee, C.F. 1999, astro-ph/9901370

Minter, A. & Spangler, S. 1997, ApJ, 485, 182

Myers, P.C. 1983, ApJ, 270, 105

Myers, P.C. 1999, in The Origin of Stars and Planetary Systems, ed. by Charles J. L. and Nikolaos D.K., Kluwer Academic Publishers, 1999, p.67

Scalo, J. M. 1984, ApJ, 277, 556

Scalo, J. M. 1987, in Interstellar Processes, ed. D. J. Hollenbach & H. A. Thronson (Dordrecht: Reidel), 349

Stanimirovic, S., & Lazarian, A. 2001, ApJ, in press